



## Performance of Savonius Turbines with Tubercles Inspired by Humpback Whales

Sohib Abdelsattar<sup>1</sup>, Nurul Asyikin Abu Bakar<sup>1</sup>, Noorfazreena Mohammad Kamaruddin<sup>1,\*</sup>

<sup>1</sup> School of Aerospace Engineering, Universiti Sains Malaysia, 14300 Nibong Tebal, Penang, Malaysia

### ARTICLE INFO

#### Article history:

Received 12 January 2023  
Received in revised form 19 May 2023  
Accepted 26 May 2023  
Available online 13 June 2023

#### Keywords:

Savonius; turbine; tubercle; experiment; power; whale

### ABSTRACT

Recent studies found that tubercles had been integrated into various applications beyond nature to enhance performance. Therefore, the present work investigates the performance of a Savonius turbine with various tubercle configurations at a wind speed of 7 m/s which corresponds to a Reynolds number of 148,000. The Savonius turbines with tubercle features were initially designed and inspired by the distribution of tubercles on the flippers of humpback whales. However, only the models with the best performance were chosen for fabrication and tested in the wind tunnel. The new turbine designs have 33% of the blade without tubercles, with turbine model 1 (D1) having a large tubercle beginning in the midspan and tapering towards the endplates, while turbine model 2 (D3) applies the 33% without tubercles in the midspan of the blade. The results demonstrated that turbine model 1 had the highest maximum  $C_p$  of 0.19 at the tip speed ratio of 0.78 and indicated that the spanwise location of tubercles in which it is integrated into the turbine is a significant geometric arrangement to improve the performance. The new turbine models designed with tubercles performed significantly better than the baseline model, with 46.15% and 23.08% improvements, respectively. The flow visualization for both models with tubercle configurations showed smaller wake sizes that represent reduced drag and eventually produced higher performance in comparison with the baseline. The results provide insights into the implementation of the tubercles concept on a Savonius turbine with a low aspect ratio.

## 1. Introduction

Tubercles are sinusoidal bumps typically found at the leading edge of the flipper of a humpback whale [1]. Many researchers have discovered that tubercles can improve flow attachment as they function similarly to flow control devices comparable to vortex generators [2-3]. This discovery sparked the development of other studies involving the application of tubercles in various fields [4-6]. Although the majority of earlier research has focused on wings and the improvement of tubercles in aerodynamic performance [7-8].

However, recent studies have been expanded to include wind turbine blades with an emphasis on the influence of leading-edge sinusoidal modifications to the blade design, which can increase

\* Corresponding author.

E-mail address: fazreena@usm.my

<https://doi.org/10.37934/araset.31.1.6878>

shaft torque in the post-stall region due to a similar working principle to vortex generators [9-10]. Unfortunately, the physical flow of tubercles is quite complex, and some researchers disagree that tubercles function as vortex generators [11]. Fish *et al.*, [12] found that the number of tubercles is typically between 9 and 11, with a greater concentration at the flipper tip than at the root. In principle, tubercles accelerate flow at troughs where the vorticity of opposite signs generates counter-rotating vortices that re-energize the boundary layer and delay flow separation [13-14].

Previous studies [15-16] demonstrated that the amplitude and wavelength of tubercles considerably impact the aerodynamic performance of a wing. However, neither study specified a method for selecting these parameters to optimize performance. Several studies discovered favorable results when small amplitude and wavelength values were employed [16] and [2], whereas others found the opposite [13]. In addition, the spanwise location of the tubercles and the termination phase are other significant geometric parameters influencing the performance [17]. In this context, the geometric parameters of tubercles were chosen randomly in most studies, making it difficult to determine the optimal amplitude and wavelength to improve the wind turbine performance. In addition, the spanwise location received less attention in comparison to other geometric parameters. This provides a gap in the research as typical wind turbine blades can be divided into three sections that contribute differently to energy production. As the second half of the blade has the most significant impact on energy output [17-18], tubercles located from the midspan to the tip may have potentially greater positive effects on improving the turbine power.

The aim of the current study is to investigate and establish a comprehensive understanding of the effect of tubercle locations on the performance of Savonius turbines at low Reynolds numbers for hydrokinetic applications. This is important as the hydrokinetic turbine is one of the alternative resources to generate sustainable energy for rural communities in Malaysia that have limited access to electricity [19-20]. The small rivers in rural areas typically have low speeds ranging from 0.2 m/s to 0.5 m/s, making it challenging to implement the Savonius turbines in this condition due to the low power efficiency [21-22] and their poor ability to self-start at low rates despite having a simple design [23-24]. Although Salleh *et al.*, [25] recently established the effectiveness of implementing deflectors into the Savonius turbine to improve power performance, this type of augmentation device adds complexity to the overall turbine configurations for practical riverside installation [26]. Therefore, it is important to conduct a more comprehensive evaluation and analysis of the effects of modifying the tubercle locations. The focus is to identify the most practical location configuration to integrate the tubercles with the combination of amplitude and wavelength characteristics in the future to enhance the performance of the turbine. This will hopefully reveal the performance of the Savonius turbine without any external augmentation devices and determine the application of tubercles to turbines other than the wing or flipper of the humpback whale. Therefore, the objectives of the work are to fabricate the Savonius turbine blade models with tubercles, and to investigate the performance of the turbine models with various tubercle configurations based on the 33% concept of the humpback whale with quantitative and qualitative measurements.

## 2. Methodology

### 2.1 The Turbine Model With Tubercles

There are a few design configurations that were constructed based on the research of Fish and Battle [27] which analyzed the location of the tubercles along the leading edge of the whale's flipper and observed that the largest tubercles started at 33% of the span. The size of the tubercles decreases as they approach the tip of the whale's flipper, eventually forming an elliptical shape that results in superior manoeuvrability. Therefore, in light of the nature of tubercles on the leading edge of the

humpback whale flipper, the same concept is applied in the current study with some modifications as described in Table 1 to adapt the practicability of turbines for hydrokinetic applications.

The new design configurations as shown in Figure 1 (D1 and D3) are mainly constructed based on the flippers of the humpback whale, focusing on the location of the tubercles integrated into the middle of the blade span. D1 is the large tubercles that started in the middle and then became smaller as they approached the endplates at the top and bottom of the edge. This results in 33% of the blade without tubercles from the endplates at the top and bottom towards the middle of the blade. The D3 design has the opposite feature of the D1 configuration, mainly constructed without tubercles in the middle of the blade span. It has large tubercles along the top and bottom edges of the end plate, which gradually diminish towards the middle of the blade span. This results in 33% of the blade being without tubercles in the middle of the blade.

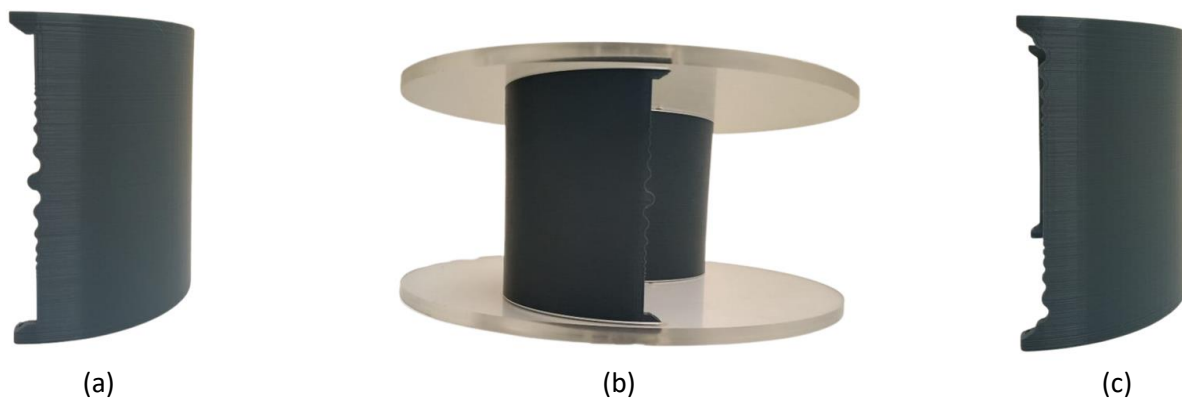


**Fig. 1.** The geometric parameters of the turbine with tubercles (a) D1, (b) the assembly of the turbine and (c) D3

**Table 1**

The dimension parameter of the turbine with tubercles

Parameters	Value (units)
Height of turbine, $H$	0.132 (m)
Diameter of turbine, $D$	0.329 (m)
Diameter of blade, $d$	0.183 (m)
Diameter of end plate, $D_E$	0.361 (m)
Thickness of blade, $t_b$	0.002 (m)
Thickness of end plate, $t_E$	0.010 (m)
Aspect ratio, $AR = H/D$	0.401

## 2.2 Experimental Setup

The turbine model with tubercles was tested in the closed-circuit wind tunnel with an incoming flow speed,  $V_\infty = 7 \text{ m/s}$ . The turbine was positioned in the middle of the wind tunnel test section as represented in Figure 2. The position of the turbine was set at a  $45^\circ$  rotor angle defined by the position of the advancing blade with respect to the incoming wind flow direction. The performance of the turbine model integrated with tubercles was determined by measuring the dynamic torque generated by the turbine, as shown in Figure 3. The Prony brake dynamometer system was positioned on top of the wind tunnel. Two load cells, a braking belt around the pulley, a hall effect sensor, and digital displays comprise the system with the load cells having an accuracy of 0.1% and a maximum load capacity of 50 N [25]. The rotation of the turbine model with tubercles was

determined by the sensor that detected the metal on the pulley. The torque was produced by detecting the force differential between the two belts and the values were captured on the digital display. The value of the differences between the two forces yields the net force value, which can be used to calculate the torque value by multiplying it by the radius of the pulley.

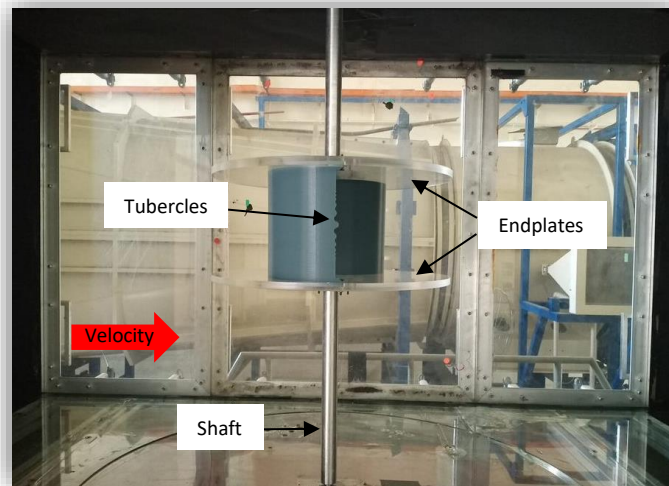


**Fig. 2.** The side view of the turbine model with tubercles in the test section

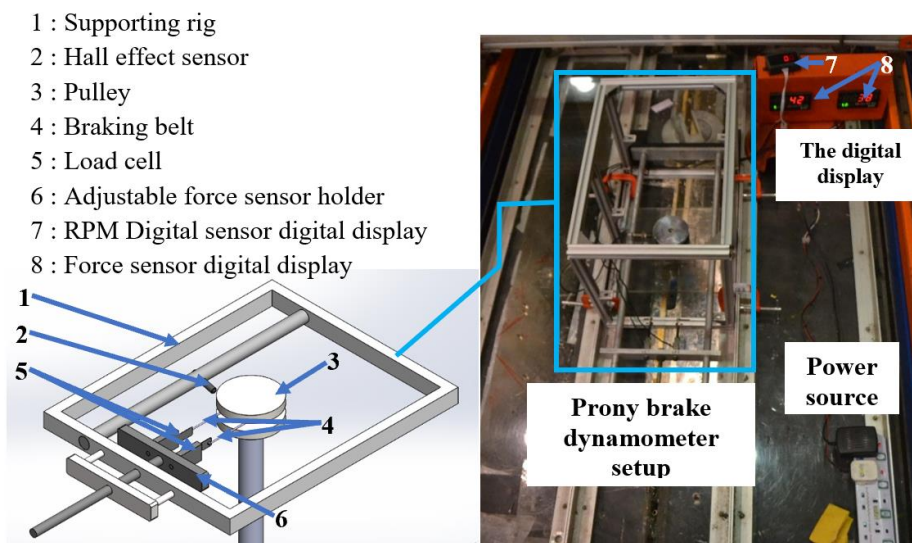


**Fig. 3.** The Prony dynamometer set up and the experimental torque setup [28]

### 2.3 Equations

The Reynolds number of 148,000 can be calculated from the wind flow speed,  $V_\infty$  with the density,  $\rho$ , and the diameter of the turbine,  $D$  as follows

$$Re = \frac{\rho U D}{\mu} \tag{1}$$

The following equation can be used to calculate the dynamic torque value from the difference in force generated from the force sensor in the tachometer,  $\Delta F$  and the radius of the pulley,  $r_p = 0.030\text{ m}$  as follows

$$T = \Delta F \times r_p \quad (2)$$

The angular speed,  $\omega$  could be calculated as follows

$$\omega = \frac{2\pi}{60} \times RPM \quad (3)$$

The rotation of the rotor, RPM was measured to obtain the angular speed,  $\omega$  of the turbine by using a non-contact digital tachometer. The coefficient of the dynamic torque can be acquired as follows

$$C_T = \frac{4T}{\rho H D^2 U^2} \quad (4)$$

By using the torque value from Eq. (2),  $\rho$  is the density of the air, H is the height of the turbine, D is the diameter of the turbine and  $V^\infty$  is the flow velocity. The value of the power coefficient was acquired from the torque value. The power available from the incoming flow,  $P_{in}$  is given by the equation below

$$P_{in} = \frac{1}{2} \rho H D U^3 \quad (5)$$

The power generated by the turbine;  $P_{out}$  is as the equation follows

$$P_{out} = T \omega \quad (6)$$

The power coefficient,  $C_p$  is calculated from the equation below

$$C_p = \frac{P_{out}}{P_{in}} \quad (7)$$

Then the power coefficient could be generated as follows

$$C_p = \frac{2T\omega}{\rho H D U^3} \quad (8)$$

The dynamic torque and power coefficient value are plotted against the tip speed ratio,  $\lambda$  where

$$\lambda = \frac{\omega D}{2U} \quad (9)$$

#### 2.4 Uncertainty Analysis

The uncertainty analysis has been calculated by using Moffat [29] from the equation below, where  $X$  is the measurement of the parameter and the  $\delta X_i$  is half of the smallest reading scale. The general uncertainty analysis is defined as follows

$$X_1 = X \pm \delta X_1 \tag{10}$$

As the  $X$  is the measurement of the parameter and the  $\delta X_i$  is half of the smallest value from the reading scale. From the above equation, the relative uncertainty is as follows

$$U_R = \pm \frac{\delta R}{R} = \left\{ \left( a \frac{\delta X_1}{X_1} \right)^2 + \left( b \frac{\delta X_2}{X_2} \right)^2 + \dots + \left( n \frac{\delta X_n}{X_n} \right)^2 \right\}^{1/2} \tag{11}$$

where the relative sensitivity coefficient is

$$a = \frac{X_1}{R} \frac{\partial R}{\partial X_1}; b = \frac{X_2}{R} \frac{\partial R}{\partial X_2}; n = \frac{X_n}{R} \frac{\partial R}{\partial X_n} \tag{12}$$

In this experiment, the uncertainty of the important parameters was the tip speed ratio, torque coefficient, and power coefficient. With all measurements, parameters were calculated using the relative sensitivity equation and included in the relative uncertainty of the tip speed ratio, the coefficient of torque, and the coefficient of power in the equation (11). Therefore, the uncertainties of all significant parameters at the maximum power coefficient at the airflow speed of 7 m/s are listed in Table 2 as follows

**Table 2**

The values of the uncertainty percentage of the parameters

Parameters	Uncertainty value		Uncertainty percentage	
	D1	D3	D1	D3
Tip speed ratio, $\lambda$	$\pm 0.0074$	$\pm 0.0076$	0.74%	0.76%
The coefficient of torque, $C_T$	$\pm 0.0225$	$\pm 0.0225$	2.25%	2.25%
The coefficient of power, $C_P$	$\pm 0.027$	$\pm 0.0276$	2.75%	2.76%

### 3. Results and Discussion

#### 3.1 The Performance of The Turbine with Tubercles

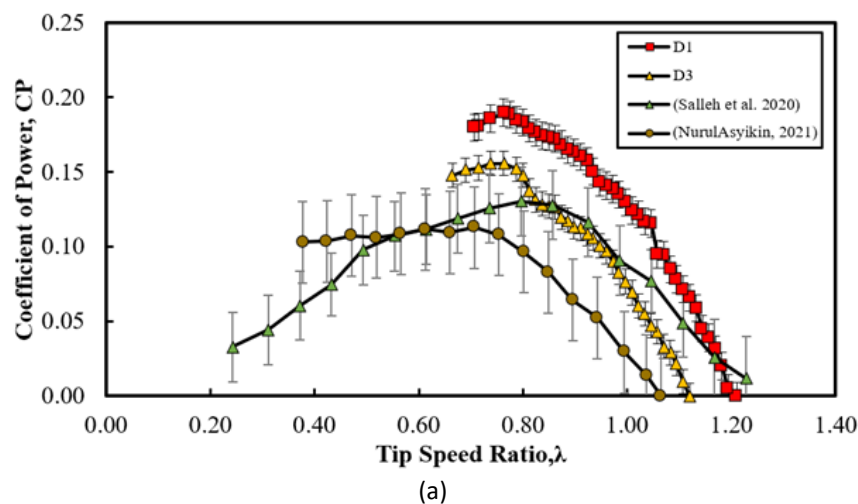
Two turbine models integrated with tubercles identified as D1 and D3 were fabricated and both models have the same exact dimensions as [30] that serve as the baseline for comparison at a Reynolds number of 148,000 which corresponds to a wind speed of 7 m/s. The comparison results for both tubercle models demonstrated an increase in performance with the D1 model having the highest maximum  $C_P$  of 0.19 at a TSR of 0.76 as depicted in Figure 4(a), and the highest maximum  $C_T$  of 0.25 at a TSR of 0.71 as shown in Figure 4(b).

The results show that the D1 model with tubercles had the highest turbine efficiency with a 46.15% improvement compared to the baseline model without any tubercles [30], while the D3 model with tubercles had a 23.08% improvement compared to the baseline as listed in Table 3. The experimental results revealed that the Savonius turbines integrated with tubercles generally have better performance. However, although both new turbine models implement the concept of 33% of the blade without tubercles as suggested by previous researchers [1,27], but the spanwise location in which this concept is implemented in the turbine plays a significant role that contributes to its superior power performance. This was demonstrated as the D1 model which was designed with large tubercles beginning in the midspan and tapering towards the top and bottom edges of the blade was more effective at enhancing the power performance than the D3 model, which had the blade without tubercles in the midspan with a maximum  $C_P$  of 0.16 at a TSR of 0.76 and a maximum  $C_T$  of 0.22 at a

TSR of 0.66. The results were consistent with the findings of [18] which emphasized the possibility of high performance improvement if tubercles are positioned from the midspan to the tip.

Previous studies have also demonstrated that leading edge tubercles generate counter-rotating vortices capable of re-energizing the boundary layer and delaying flow separation which consequently enhances performance [14,16]. This most likely explains the reason the turbine model with tubercles in the present study possessed superior performance despite being tested at a low Reynolds number. However, the formation of counter-rotating vortices that exhibit comparable behavior to that of a vortex generator previously mentioned [7] could not be captured now because the current work is limited to quantitative measurements. These physical vortex phenomena could be verified using qualitative measurements that are capable of capturing the flow surrounding the turbines.

Figure 4 shows the performance comparison between fabricated tubercle models and the baseline [30] without tubercles. As mentioned previously, the conventional 2-bladed Savonius turbine was selected to serve as a baseline for comparison with the current study because the Reynolds number of 148,000 is similar to the present study with the same aspect ratio of 0.4. The wind tunnel experiments were conducted at 7 m/s equivalent to a water flow speed of 0.4 m/s. The results highlighted that the turbine with tubercles in the present study could be implemented for hydrokinetic applications due to the similarity between wind and water flow [25]. In addition, the results were also compared to the hybrid turbine of Abu Bakar [28] with a maximum  $C_p$  of 0.11 at a TSR of 0.71, because it has the same aspect ratio of 0.4 as the present study, although the Reynolds number was slightly higher at 157, 000. It highlights the superior performance of the turbine with tubercles, particularly the D1 model, with a 42.11% improvement in power coefficient compared to the hybrid model, despite having a relatively low Reynolds number. Although [30-33] found that the power coefficient increased with the increasing Reynolds number, a comparison between the present study and Abu Bakar [28] revealed the turbine with tubercles performed better even at a low Reynolds number.



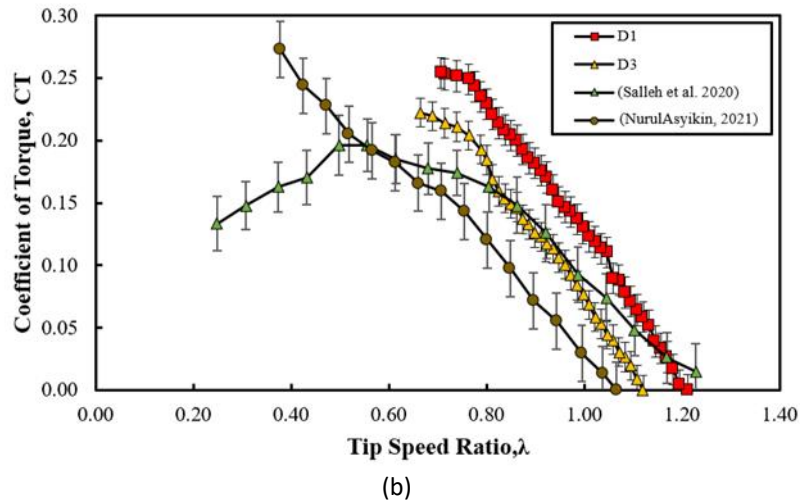


**Fig. 4.** (a) The torque coefficient and (b) The power coefficient of the turbine

**Table 3**

The comparison data of the baseline and turbine models with tubercles

Author	Reynolds number	Tip speed ratio, $\lambda$	Maximum torque coefficient, CT	Maximum power coefficient, CP	Performance comparison with respect to baseline (%)
Salleh <i>et al.</i> , [30]	148 000	0.80	0.20	0.13	-
D3	148 000	0.76	0.22	0.16	23.08
D1	148 000	0.78	0.25	0.19	46.15

Furthermore, the smoke flow visualization image captured to illustrate the top view flow structure of the turbine with tubercles as shown in Figure 5 indicated clear streamlines upstream and a small wake region downstream generated behind the rotating turbine. The small wake size represents less pressure drag which results in an increment in the performance of the turbine with tubercles compared to the baseline without tubercles.

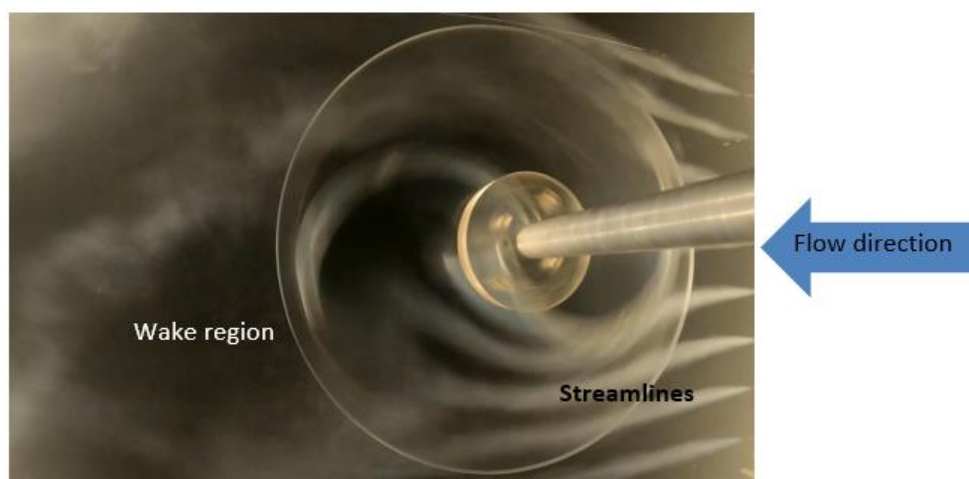


**Fig. 5.** The top view flow visualization of the turbine with tubercles

## 4. Conclusions

The two turbine models with tubercles identified as D1 and D3 showed outstanding power performance. Both designs implement the concept of 33% of the blade without tubercles, although the locations are varied either in the midspan or near the tip. D1 was designed with large tubercles starting in the middle and then reducing to smaller ones as they approached the endplates at the top and bottom of the edge, while the concept of 33% of the blade without tubercles was implemented in the middle of the blade for D3. The results revealed that the spanwise location of tubercles integrated into the turbine is a critical geometric configuration that must be considered when analyzing the performance of turbines. This is because the tubercles are not equally distributed along the flipper span of the humpback whales, as they begin at around 33% of the span and become smaller near the tip. The D1 turbine model performed the best at a tip speed ratio of 0.78 with a maximum power coefficient of 0.19 and torque coefficient of 0.25, respectively. This is followed by the D3 model with a maximum power coefficient of 0.16 and a torque coefficient of 0.22 at a tip speed ratio of 0.76. Both designs D1 and D3 integrated with tubercles outperformed the baseline model without tubercles with relatively small wake sizes as illustrated in flow visualization measurement, with a 46.15% and 23.08% improvement, respectively.

### Credit Authorship Contribution Statement

Sohib Abdelsattar: Investigation, Methodology, Formal analysis, Writing - original draft. Nurul Asyikin Abu Bakar: Methodology, Formal analysis. Noorfazreena M. Kamaruddin: Conceptualization, Methodology, Formal analysis, Writing – review & editing, Supervision, Project administration.

### Declaration of Competing Interest

The authors declare that they have no known competing financial interests or personal relationships that could have appeared to influence the work reported in this paper.

### Acknowledgment

The authors would like to acknowledge the financial support from the Ministry of Higher Education Malaysia, under the Fundamental Research Grant Scheme: (FRGS/1/2022/TK08/USM/03/3).

### References

- [1] Watts, Phil, and Frank E. Fish. "The influence of passive, leading edge tubercles on wing performance." In *Proc. Twelfth Intl. Symp. Unmanned Untethered Submers. Technol.* Durham New Hampshire: Auton. Undersea Syst. Inst., 2001.
- [2] Johari, Hamid, Charles Henoah, Derrick Custodio, and Alexandra Levshin. "Effects of leading-edge protuberances on airfoil performance." *AIAA journal* 45, no. 11 (2007): 2634-2642. <https://doi.org/10.2514/1.28497>
- [3] Hansen, Kristy L., Nikan Rostamzadeh, Richard M. Kelso, and Bassam B. Dally. "Evolution of the streamwise vortices generated between leading edge tubercles." *Journal of Fluid Mechanics* 788 (2016): 730-766. <https://doi.org/10.1017/jfm.2015.611>
- [4] Huang, Guo-Yuan, Y. C. Shiah, Chi-Jeng Bai, and W. T. Chong. "Experimental study of the protuberance effect on the blade performance of a small horizontal axis wind turbine." *Journal of Wind Engineering and Industrial Aerodynamics* 147 (2015): 202-211. <https://doi.org/10.1016/j.jweia.2015.10.005>
- [5] Kumar, Yogesh, Jordan Ringenberg, Soma Shekara Depuru, Vijay K. Devabhaktuni, Jin Woo Lee, Efstratios Nikolaidis, Brett Andersen, and Abdollah Afjeh. "Wind energy: Trends and enabling technologies." *Renewable and Sustainable Energy Reviews* 53 (2016): 209-224. <https://doi.org/10.1016/j.rser.2015.07.200>
- [6] Stark, Callum, and Weichao Shi. "The influence of leading-edge tubercles on the sheet cavitation development of a benchmark marine propeller." In *International Conference on Offshore Mechanics and Arctic Engineering*, vol. 85161, p. V006T06A025. American Society of Mechanical Engineers, 2021. <https://doi.org/10.1115/OMAE2021-62292>

- [7] Murray, M. M., D. S. Miklosovic, F. E. Fish, and L. E. Howle. "Effects of leading edge tubercles on a representative whale flipper model at various sweep angles." In *Durham, NH: Conference Proceedings of the 14th International Symposium on Unmanned Untethered Submersible Technology*. 2005.
- [8] Carreira Pedro, Hugo, and Marcelo Kobayashi. "Numerical study of stall delay on humpback whale flippers." In *46th AIAA aerospace sciences meeting and exhibit*, p. 584. 2008. <https://doi.org/10.2514/6.2008-584>
- [9] Shi, Weichao, Mehmet Atlar, Roslyna Rosli, Batuhan Aktas, and Rosemary Norman. "Cavitation observations and noise measurements of horizontal axis tidal turbines with biomimetic blade leading-edge designs." *Ocean engineering* 121 (2016): 143-155. <https://doi.org/10.1016/j.oceaneng.2016.05.030>
- [10] Shi, Weichao, Mehmet Atlar, and Rosemary Norman. "Detailed flow measurement of the field around tidal turbines with and without biomimetic leading-edge tubercles." *Renewable Energy* 111 (2017): 688-707. <https://doi.org/10.1016/j.renene.2017.04.053>
- [11] Van Nierop, Ernst A., Silas Alben, and Michael P. Brenner. "How bumps on whale flippers delay stall: an aerodynamic model." *Physical review letters* 100, no. 5 (2008): 054502. <https://doi.org/10.1103/PhysRevLett.100.054502>
- [12] Fish, Frank E., Paul W. Weber, Mark M. Murray, and Laurens E. Howle. "The tubercles on humpback whales' flippers: application of bio-inspired technology." (2011): 203-213. <https://doi.org/10.1093/icb/icr016>
- [13] Weber, Paul W., Laurens E. Howle, and Mark M. Murray. "Lift, drag, and cavitation onset on rudders with leading-edge tubercles." *Marine Technology and SNAME News* 47, no. 01 (2010): 27-36. <https://doi.org/10.5957/mtsn.2010.47.1.27>
- [14] Hansen, Kristy Lee. "Effect of leading edge tubercles on airfoil performance." PhD diss., 2012.
- [15] Zhang, R. K., and V. D. Wu. "JZ, 2011," "Aerodynamic Characteristics of Wind Turbine Blades with a Sinusoidal Leading Edge." *Wind Energy*. <https://doi.org/10.1002/we.479>
- [16] Hansen, Kristy L., Nikan Rostamzadeh, Richard M. Kelso, and Bassam B. Dally. "Evolution of the streamwise vortices generated between leading edge tubercles." *Journal of Fluid Mechanics* 788 (2016): 730-766. <https://doi.org/10.1017/jfm.2015.611>
- [17] Bolzon, Michael D., Richard M. Kelso, and Maziar Arjomandi. "Tubercles and their applications." *Journal of aerospace engineering* 29, no. 1 (2016): 04015013. [https://doi.org/10.1061/\(ASCE\)AS.1943-5525.0000491](https://doi.org/10.1061/(ASCE)AS.1943-5525.0000491)
- [18] Abate, Giada. "A numerical investigation into the aerodynamic effects of tubercles in wind turbine blades." PhD diss., Georgia Institute of Technology, 2019.
- [19] Borhanazad, Hanieh, Saad Mekhilef, R. Saidur, and G. Boroumandjazi. "Potential application of renewable energy for rural electrification in Malaysia." *Renewable energy* 59 (2013): 210-219. <https://doi.org/10.1016/j.renene.2013.03.039>
- [20] Salleh, Mohd Badrul, Noorfazreena M. Kamaruddin, and Zulfaa Mohamed-Kassim. "Savonius hydrokinetic turbines for a sustainable river-based energy extraction: A review of the technology and potential applications in Malaysia." *Sustainable energy technologies and assessments* 36 (2019): 100554. <https://doi.org/10.1016/j.seta.2019.100554>
- [21] Hossain, Farhad M., Mohammad Hasanuzzaman, N. A. Rahim, and H. W. Ping. "Impact of renewable energy on rural electrification in Malaysia: a review." *Clean Technologies and Environmental Policy* 17 (2015): 859-871. <https://doi.org/10.1007/s10098-014-0861-1>
- [22] Samsudin, Mohamed Syahril Nazreen, M. M. Rahman, and Mazlan Abdul Wahid. "Power generation sources in Malaysia: Status and prospects for sustainable development." *Journal of Advanced Review on Scientific Research* 25, no. 1 (2016): 11-28.
- [23] Alom, Nur, and Ujjwal K. Saha. "Four decades of research into the augmentation techniques of Savonius wind turbine rotor." *Journal of Energy Resources Technology* 140, no. 5 (2018). <https://doi.org/10.1115/1.4038785>
- [24] Alizadeh, Hossein, Mohammad Hossein Jahangir, and Roghayeh Ghasempour. "CFD-based improvement of Savonius type hydrokinetic turbine using optimized barrier at the low-speed flows." *Ocean Engineering* 202 (2020): 107178. <https://doi.org/10.1016/j.oceaneng.2020.107178>
- [25] Salleh, Mohd Badrul, Noorfazreena M. Kamaruddin, and Zulfaa Mohamed-Kassim. "The effects of a deflector on the self-starting speed and power performance of 2-bladed and 3-bladed Savonius rotors for hydrokinetic application." *Energy for Sustainable Development* 61 (2021): 168-180. <https://doi.org/10.1016/j.esd.2021.02.005>
- [26] Basumatary, Mithinga, Agnimitra Biswas, and Rahul Dev Misra. "Experimental verification of improved performance of Savonius turbine with a combined lift and drag based blade profile for ultra-low head river application." *Sustainable Energy Technologies and Assessments* 44 (2021): 100999. <https://doi.org/10.1016/j.seta.2021.100999>
- [27] Fish, Franke E., and Juliann M. Battle. "Hydrodynamic design of the humpback whale flipper." *Journal of morphology* 225, no. 1 (1995): 51-60. <https://doi.org/10.1002/jmor.1052250105>
- [28] Abu Bakar, Nurul Asyikin. "Experimental Investigation on the Flow Structure of a Hybrid Turbine for hydrokinetic application", Final Year Project thesis, Universiti Sains Malaysia, 2021.

- [29] Moffat, Robert J. "Describing the uncertainties in experimental results." *Experimental thermal and fluid science* 1, no. 1 (1988): 3-17. [https://doi.org/10.1016/0894-1777\(88\)90043-X](https://doi.org/10.1016/0894-1777(88)90043-X)
- [30] Salleh, Mohd Badrul, Noorfazreena M. Kamaruddin, and Zulfaa Mohamed-Kassim. "The effects of deflector longitudinal position and height on the power performance of a conventional Savonius turbine." *Energy Conversion and Management* 226 (2020): 113584. <https://doi.org/10.1016/j.enconman.2020.113584>
- [31] Shamsuddin, Muhd Syukri Mohd, Nujjiya Abdul Mu'in, and Noorfazreena Mohammad Kamaruddin. "Experimental Investigation of the Savonius Turbine for Low-Speed Hydrokinetic Applications in Small Rivers." *Journal of Advanced Research in Fluid Mechanics and Thermal Sciences* 94, no. 2 (2022): 29-46. <https://doi.org/10.37934/arfmts.94.2.2946>
- [32] Bakar, Nurul Asyikin Abu, Muhd Syukri Mohd Shamsuddin, and Noorfazreena M. Kamaruddin. "Experimental Study of a Hybrid Turbine for Hydrokinetic Applications on Small Rivers in Malaysia." *Journal of Advanced Research in Applied Sciences and Engineering Technology* 28, no. 2 (2022): 318-324. <https://doi.org/10.37934/araset.28.2.318324>
- [33] Halmy, Muhammad Syahmy Mohd, Djamel Hissein Didane, Lukmon Owolabi Afolabi, and Sami Al-Alimi. "Computational Fluid Dynamics (CFD) Study on the Effect of the Number of Blades on the Performance of Double-Stage Savonius Rotor." *Cfd Letters* 13, no. 4 (2021): 1-10. <https://doi.org/10.37934/cfdl.13.4.110>